Projection onto Convex Sets Method in Space-frequency Domain for Super Resolution

Wanqiang Shen
School of Science, Jiangnan University, Wuxi, China
Email: wq_shen@163.com

Lincong Fang
School of Information Technology, Zhejiang University of Finance & Ecnomics, Hangzhou, China
Email: lincongfang@gmail.com

Xiang Chen and Honglin Xu
School of Science, Jiangnan University, Wuxi, China
Email: {chenxiang204@gmail.com and xuhonglin@jiangnan.edu.cn}

***Abstract*—The aim of super resolution is to get high resolution (HR) images/videos from low-resolution (LR) images/videos. The obtained HR images/videos are expected to be clear and have less artifacts. Projection Onto Convex Sets (POCS) in the space domain is a super resolution method. It results in edge oscillation and produces many artifacts. This paper introduces a POCS method in both the space and the frequency domain. Firstly, a frequency domain POCS method is proposed. Then it is combined with the space POCS and the space-frequency POCS is obtained. Compared with the common bilinear interpolation method and the existing POCS method in the space domain, our method may decrease the edge oscillation phenomena and raise the Peak Signal to Noise Ratio (PSNR).**

***Index Terms*—super-resolution, Projection Onto Convex Sets (POCS), space-frequency domain, edge oscillation, Peak Signal to Noise Ratio (PSNR)**

I. INTRODUCTION

It is easy for people to get digital images and videos from various channels in today's society. However, the existing resolutions of these digital elements may not meet the requirements of people usually. One way to raise the resolutions is to update the hard devices. It often requires a high cost. The other way is to use software. It creates high resolution (HR) images/videos from Low resolution (LR) ones. This process is called super-resolution. It is widely used in the fields of intelligent surveillance [1, 2], remote sensing [3], medical technology [4], mobile devices [5], and so on.

There are a lot of super resolution methods. These methods are mainly divided into two classes [6]. The first is based on learning. In 2002, Reference [7] uses a nearest-neighbor search in the training set to get a one-pass super resolution algorithm. Reference [8] uses contourlet transformation for video super-resolution. In 2010, Reference [9] combines the partial differential equations' regularization with the learning-based super-resolution process. Reference [10] uses nonlinear mappings to coherent features and recognizes the faces in the LR images. In the train set, Reference [11] uses the kernel partial least square to describe the relationship between the LR and the HR images. The second is based on reconstruction. The HR images are reconstructed as the inverses of the LR images in these methods, such as interpolation [12-15], Projection onto Convex Sets (POCS) [16-18], Maximum a Posteriori [19-22], Iterative Back Projection [23-25], and their combination [26].

In this paper, we focus on the conventional POCS method in the space domain. It uses a priori knowledge, and is easy for implementing [27]. However, its reconstructed images may have edge oscillations. We will give a space-frequency POCS instead. By using our method, the edge oscillation phenomena will be decreased, and the Peak Signal to Noise Ratio (PSNR) will be increased.

The rest of the paper is divided into 4 parts. In the next section, the conventional POCS is introduced shortly. Section 3 and Section 4 shows our method for images and videos, respectively. The final conclusions are drawn in the last section.

II. POCS METHOD

In this section, we will overview the conventional POCS method [16] shortly.

The principle of the POCS method is simple and direct to view. It uses a priori knowledge of the spatial response characteristics of the imaging system. In the process of reconstructing HR image, there are many constraints. All the constraints, regarded as the boundaries, build a set. The set is made up of some convex sets with good

Corresponding author: Wanqiang Shen

© 2014 ACADEMY PUBLISHER
doi:10.4304/jcp.9.8.1959-1966

properties. This is the solution space of the HR images. Then the required HR image is the optimal solution in the space, that is, the projections onto the convex sets. So the main idea of POCS is to solve a constrained optimization problem.

See Fig. 1. There should be the minimal residuals between the given images and the LR images degenerated by the required HR image. This is the target function in the constrained optimization problem.

The constraints are described as that if the residuals are all less than a given threshold, then the projections from the HR image to the LR ones are obtained; otherwise, the degenerating model is needed to be modified. Both the target function and the constraints are described in the space domain. So we call it space POCS in this paper.

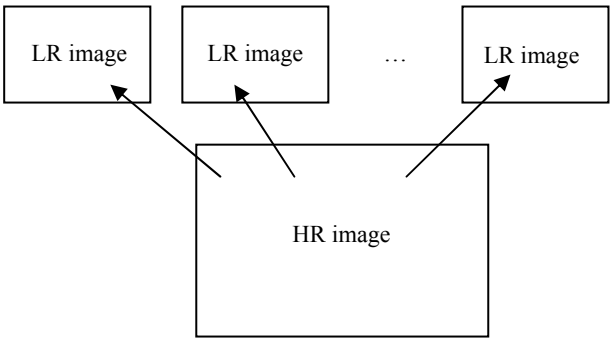

Figure 1. Explanation of POCS method.

III. Space-Frequency POCS For IMAGEs

In this section, we use our space-frequency POCS for image super resolution. The first subsection deals with the image matching process. In the second subsection, our POCS in the frequency domain is introduced. The third subsection combines the space and the frequency domain and gets our space-frequency POCS. We also give examples to show visual comparisons among the bilinear interpolation, the space POCS and our space-frequency POCS. In the last subsection, we give the PSNR as a quantitative comparison of the above mentioned three methods.

We firstly use bilinear interpolation, a simple and common method, to get a HR reference image, noted as $f(x,y)$, where x and y is corresponding to the row and the column number of pixels, respectively.

A. Image Matching

There are many images matching method. In this paper, we hope to effectively describe the rotation, translation and scaling movements between two images caused by relative motion between the lens and the scene. Moreover, the method is expected to be used in video cases easily. So we choose the least square image matching based on affine models [28].

Given a reference image $I_0(x,y)$, the matched image $I_1(x,y)$, can be presented thought the affine relations as follows.

$$I_1(x,y)=I_0(x_0,y_0)=I_0(x+(a_x+b_x x+c_x y),y+(a_y+b_y x+c_y y)) \quad (1)$$

where $a_x, b_x, c_x, a_y, b_y, c_y$ are the parameters of the affine transformation. Then the square error of the two images is

$$E(a_x,b_x,c_x,a_y,b_y,c_y)=\sum_{(x,y)}\left[I_1(x,y)-I_0(x_0,y_0)\right]^2. \quad (2)$$

Least square matching of the two images is the process of solving the parameters for the minimal E. That is,

$$\arg\min_{a_x,b_x,c_x,a_y,b_y,c_y} = E(a_x,b_x,c_x,a_y,b_y,c_y). \quad (3)$$

In the neighborhood of the pixel (x,y), we use the Taylor expansion to approximate $I_0(x_0,y_0)$.

$$\begin{aligned} &I_0(x_0,y_0)\approx I_0(x,y)\\ &+(a_x+b_x x+c_x y)d_x(x,y)+(a_y+b_y x+c_y y)d_y(x,y), \end{aligned} \quad (4)$$

where

$$d_x(x,y)=\frac{\partial I_0(x,y)}{\partial x}=\frac{1}{2}\left[I_0(x+1,y)-I_0(x-1,y)\right] \quad (5)$$

and

$$d_y(x,y)=\frac{\partial I_0(x,y)}{\partial y}=\frac{1}{2}\left[I_0(x,y+1)-I_0(x,y-1)\right] \quad (6)$$

separately denotes the gradient of $I_0(x,y)$ along the x and y direction.

Let

$$\Delta I(x,y)=I_1(x,y)-I_0(x,y). \quad (7)$$

Then the problem (3) can be represented as

$$\sum_{(x,y)} 2\left[q(x,y)^T p-\Delta I(x,y)\right]q(x,y)=0 \quad (8)$$

where

$$q=\left[d_x \quad xd_x \quad yd_x \quad d_y \quad xd_y \quad yd_y\right]^T \quad (9)$$

is the coefficient matrix and

$$p=\left[a_x \; b_x \; c_x \; a_y \; b_y \; c_y\right]^T \quad (10)$$

is the parameter vector. The iterative process is

$$\begin{bmatrix} 1 & 0 & 0 \\ a_x^{\,i+1} & b_x^{\,i+1} & c_x^{\,i+1} \\ a_y^{\,i+1} & b_y^{\,i+1} & c_y^{\,i+1} \end{bmatrix} = \begin{bmatrix} 1 & 0 & 0 \\ \Delta a_x^{\,i} & 1+\Delta b_x^{\,i} & \Delta c_x^{\,i} \\ \Delta a_y^{\,i} & \Delta b_y^{\,i} & 1+\Delta c_y^{\,i} \end{bmatrix} \begin{bmatrix} 1 & 0 & 0 \\ a_x^{\,i} & b_x^{\,i} & c_x^{\,i} \\ a_y^{\,i} & b_y^{\,i} & c_y^{\,i} \end{bmatrix}. \quad (11)$$

The Matlab program for calculating the affine parameters can be seen in Appendix A. We use small sampling level here. This estimation applies to the small amplitude of movement, which is enough for our examples in this paper. If more accurate estimation of the successive correction parameters is need, then more iterative steps may be used.

© 2014 ACADEMY PUBLISHER

B. POCS in Frequency Domain

The conventional POCS is in the space domain. This subsection will give a POCS in the frequency domain. We call it frequency POCS. Different from [17], we focus on the norm in the frequency domain.

We use the Gauss function, a very common degrading function in many optical systems, as the Point Spread Function (PSF).

$$h(x_0, y_0) = Ce^{\frac{(x-x_0)^2+(y-y_0)^2}{2\sigma^2}}, \quad (12)$$

where (x_0, y_0) is the spread center and σ denotes the blurring level of the image. C is the constant to normalize the function. It fulfills

$$\sum_{x-x_0=-w}^{x-x_0=w}\sum_{y-y_0=-w}^{y-y_0=w} h(x_0, y_0) = 1, \quad (13)$$

where w gives the radius of the support domain of the PSF.

We assume that $g_k(i, j)$ denotes the observed kth LR images. According to the motion vector field, for each pixel $g_k(i_0, j_0)$ in $g_k(i, j)$, we can get the corresponding coordinate of the point in $f(x, y)$, the reference image. The point is noted as $f(x_0, y_0)$. Then the estimated LR image is regarded as the image degenerated from the HR image through the Gauss blurring. That is,

$$\hat{g}_k(i_0, j_0) = \sum_{x-x_0=-w}^{x-x_0=w}\sum_{y-y_0=-w}^{y-y_0=w} h(x_0, y_0) f(x_0, y_0) \quad (14)$$

The residual between the estimated and the observed LR images can be given by the following formula.

$$r(x_0, y_0) = g_k(i_0, j_0) - \hat{g}_k(i_0, j_0) \ . \quad (15)$$

If $f(x, y)$ is the ideal HR images, then the residual $r(x, y)$ is equal to zero. Let δ_0 be a positive number. It is used as a threshold to construct the iterative function. If the residual r is in the threshold range, then $f(x, y)$ will be unchanged, otherwise, $f(x, y)$ will be modified. If r is too small or too large, then it will be increased or decreased until it is near-zero, i.e. in the δ_0 determined neighborhood of zero. The iterative process can be presented as follows.

$$P[f(x_0, y_0)] = \begin{cases} f(x_0, y_0) + u(r + \delta_0)h(x_0, y_0) & r < -\delta_0 \\ f(x_0, y_0) & -\delta_0 \le r \le \delta_0 \\ f(x_0, y_0) + u(r - \delta_0)h(x_0, y_0) & r > \delta_0 \end{cases}, \quad (16)$$

where u is a constant to control the convergence speed of the iterative process.

The above three formulas, (14), (15) and (16) are all in the space domain. They are used in the space POCS method. We use the Fourier transformation, a common technique, to change them into the frequency domain. In the frequency POCS, our estimated LR image is presented as follows.

$$F(\hat{g}_k(i_0, j_0)) = \sum_{x-x_0=-w}^{x-x_0=w}\sum_{y-y_0=-w}^{y-y_0=w} F(h(x_0, y_0)) * F(f(x_0, y_0)), \quad (17)$$

where F is the Fourier transformation, and "*" means the convolution operator. Then our residual in the frequency domain is

$$R = \left\| F(g_k(i_0, j_0)) - F(\hat{g}_k(i_0, j_0)) \right\|. \quad (18)$$

Analogously, our iterative process in the frequency domain is presented as

$$\left\| P\left[F(f(x_0, y_0)) \right] \right\| = \begin{cases} \left\| F(f(x_0, y_0)) \right\| & \\ +u(R + \delta)\left\| F(f(x_0, y_0)) \right\| & R < -\delta \\ \left\| F(f(x_0, y_0)) \right\| & |R| \le \delta \\ \left\| F(f(x_0, y_0)) \right\| & \\ +u(R - \delta)\left\| F(f(x_0, y_0)) \right\| & R > \delta \end{cases}, \quad (19)$$

where δ is a threshold.

By now, we have two POCS models. One is in the space domain, and the other is in the frequency domain. Then we will combine them with each other in the next subsection.

C. Combining Space and Frequency POCS

Assume that the HR image obtained by using the space POCS and the frequency POCS is $s(x, y)$ and $f(x, y)$, respectively. Then we use an interpolation method to get the final HR image.

$$G(x, y) = \alpha(x, y)s(x, y) + (1 - \alpha(x, y))f(x, y), \quad (20)$$

where $\alpha(x, y)$ is the interpolation function defined by

$$\alpha(x, y) = \begin{cases} 0, & (x, y) \in W \\ 1, & (x, y) \notin W \end{cases}, \quad (21)$$

and W is the edge set of the image which may be obtained by an algorithm of edge detection, for example, Canny detection.

To see the super-resolution effects of our method, we give two examples for images. In this paper, we assume that the pixels' size do not changed in the super resolution process. So, raising resolution means the size of image/video increased. In all the examples of the paper, the original LR images/videos are all with smaller size, and the super-resolution HR images/videos are all with bigger size.

Fig. 2 shows the first example. Fig. 2(a) is the LR image with the resolution 176×144. Fig. 2(b), Fig. 2(c), Fig. 2(e) is the obtained HR image with the resolution 352×288 by the bilinear interpolation, the traditional space POCS and our space-frequency POCS, respectively.

It is easy for us to see that Fig. 2(c) and Fig. 2(e) are both clearer than Fig. 2(b). However, the difference between Fig. 2(c) and Fig. 2(e) is not obvious. So we magnify the same region of Fig. 2(c) and Fig. 2(e) to the same 800% times. The region is bounded by a blue box in Fig. 2(c) and Fig. 2(e), separately. The magnified region corresponding to Fig. 2(c), Fig. 2(e) is Fig. 2(d), Fig. 2(f), respectively.

© 2014 ACADEMY PUBLISHER

By contrast, we can see that the light spots in Fig. 2(e) are clearer than those in Fig. 2(d).

(a) Original LR image. (b) Bilinear interpolation method.

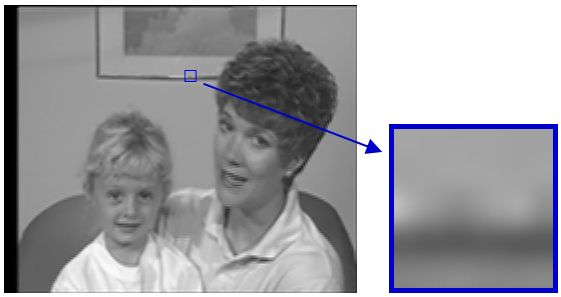

(c) Space POCS method. (d) Magnified region in (c).

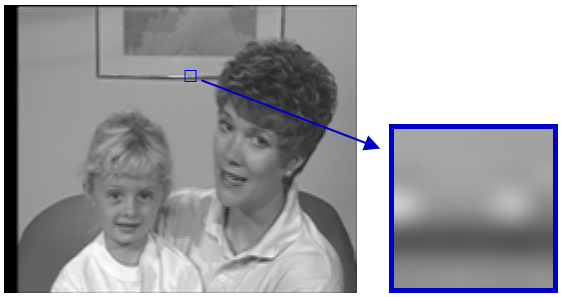

(e) Our method. (f) Magnified region in (e).

Figure 2. Image Ex. 1.

Fig. 3 gives the second example. Fig. 3(a) is the LR image with the resolution 176×144. Fig. 3(b), Fig. 3(c), Fig. 3(e) is the obtained HR image with the resolution 352×288 by the bilinear interpolation, the traditional space POCS and our space-frequency POCS, respectively.

It is easy for us to see that Fig. 3(c) and Fig. 3(e) are both clearer than Fig. 3(b). However, the difference between Fig. 3(c) and Fig. 3(e) is not obvious. So we magnify the same region of Fig. 3(c) and Fig. 3(e) to the same 800% times. The region is bounded by a blue box in Fig. 3(c) and Fig. 3(e), separately. The magnified region corresponding to Fig. 3(c), Fig. 3(e) is Fig. 3(d), Fig. 3(f), respectively.

In Fig. 3(d), we can see many black stripes, especially in the edge of the red region. These stripes are all artifacts. They make the edge seems to be wider and oscillating. Our method decreases the phenomena, seen in Fig. 3(f).

Comparing the conventional space POCS method with our space-frequency POCS method from vision effects, we can get the result that our method may decrease the edge oscillation phenomena and artifacts produced by the conventional POCS method and make the image clearer.

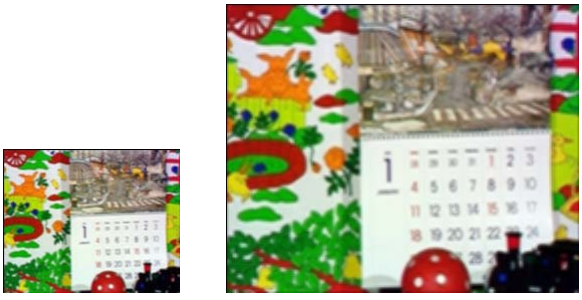

(a) Original LR image. (b) Bilinear interpolation method.

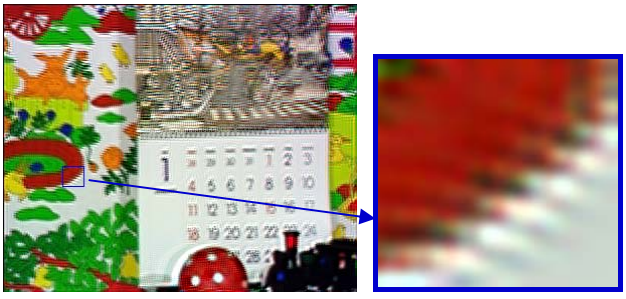

(c) Space POCS method. (d) Magnified region in (c).

(e) Our method. (f) Magnified region in (e).

Figure 3. Image Ex. 2.

D. PSNR

In the last subsection, we show some visual results. In this subsection, a quantitative comparison among the bilinear interpolation, the traditional POCS method and our method will be given. We use PSNR to describe the quality of the super-resolution reconstruction.

$$PSNR = 10\log\left(\frac{255^2}{MSE}\right), \tag{22}$$

where MSE is the mean square error defined as

$$MSE = \frac{\sum_{y=1}^{y=n}\sum_{x=1}^{x=m}\left(f(x,y)-f'(x,y)\right)^2}{m\times n}, \tag{23}$$

and $f(x, y), f'(x, y)$ is separately the real HR image and the HR image obtained by using some algorithm. m and n is the horizontal and vertical resolution, respectively.

Consider the examples in the last subsection. Their PSNR by using the bilinear interpolation, the traditional

© 2014 ACADEMY PUBLISHER

POCS and our method is listed in Table 1. From this table, we can see that in the two examples, the PSNRs of our method are greater than those of the conventional POCS and the bilinear interpolation approach.

TABLE I.
COMPARISON OF PSNR

Ex.	PSNR(dB)		
	Bilinear interpolation	Space POCS	Our method
1	28.29	28.99	29.42
2	17.72	18.43	18.73

IV. SPACE-FREQUENCE POCS FOR VIDEOS

We can use the similar method for video super-resolution. Motion estimation is dealt with in the process of image matching. For any frame in the video, we use the previous frame to solve the affine model, and use the current frame to modify the parameters of the model. The process is shown in Fig. 4.

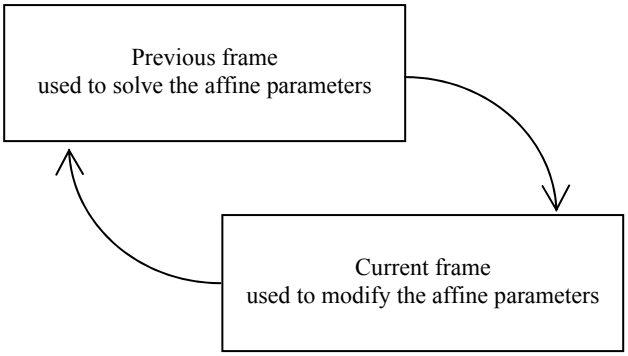

Figure 4. Explanation of affine model.

See examples. Fig. 5 shows the first video example consisted of three neighbor frames. The space resolution of the given LR video is 176×144. After super resolution, the row and column resolutions are both doubled. The HR video produced by our method is with the space resolution 352×288.

Fig. 5(a), Fig. 5(b) and Fig. 5(c) are the given LR frames, where Fig. 5(b) is the current *i*th frame, Fig. 5(a) is the pervious (*i*-1)th frame, and Fig. 5(c) is the next (*i*+1)th frame.

Fig. 5(d), Fig. 5(e) and Fig. 5(f) are the HR frames constructed by our space-frequency POCS method. They are corresponding to Fig. 5(a), Fig. 5(b) and Fig. 5(c) in order. So the frame number of Fig. 5(d), Fig. 5(e) and Fig. 5(f) is the same as Fig. 5(a), Fig. 5(b) and Fig. 5(c), i.e. *i*-1, *i*, *i*+1, respectively.

Fig. 6 gives another video example. It shows the nonadjacent video frames. The space resolution of the given LR video and the HR video is also 176×144 and 352×288, respectively. The HR video is constructed by using our method.

Fig. 6(a), Fig. 6(b) and Fig. 6(c) are the given LR frames. They are nonadjacent. The frame number of Fig. 6(a), Fig. 6(b) and Fig. 6(c) is assumed as *i*, *j* and *k*, respectively.

Fig. 6(d), Fig. 6(e) and Fig. 6(f) are the HR frames constructed by our space-frequency POCS method. The frame number of Fig. 6(d), Fig. 6(e) and Fig. 6(f) is *i*, *j* and *k*, respectively. This means that Fig. 6(d), Fig. 6(e) and Fig. 6(f) is the HR frame corresponding to Fig. 6(a), Fig. 6(b) and Fig. 6(c), respectively.

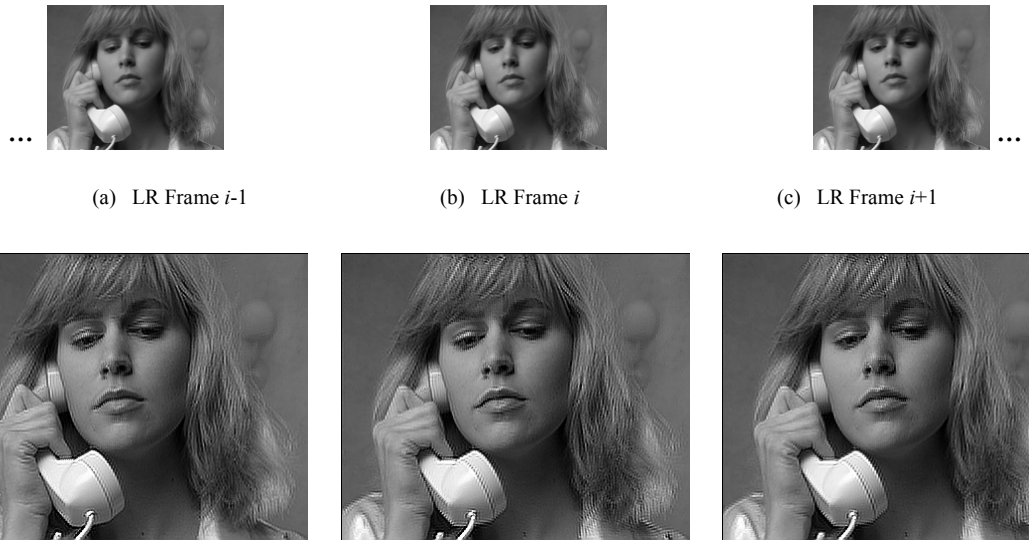

(a) LR Frame *i*-1 (b) LR Frame *i* (c) LR Frame *i*+1

(d) HR Frame *i*-1 (e) HR Frame *i* (f) HR Frame *i*+1

Figure 5. Video Ex. 1.

© 2014 ACADEMY PUBLISHER

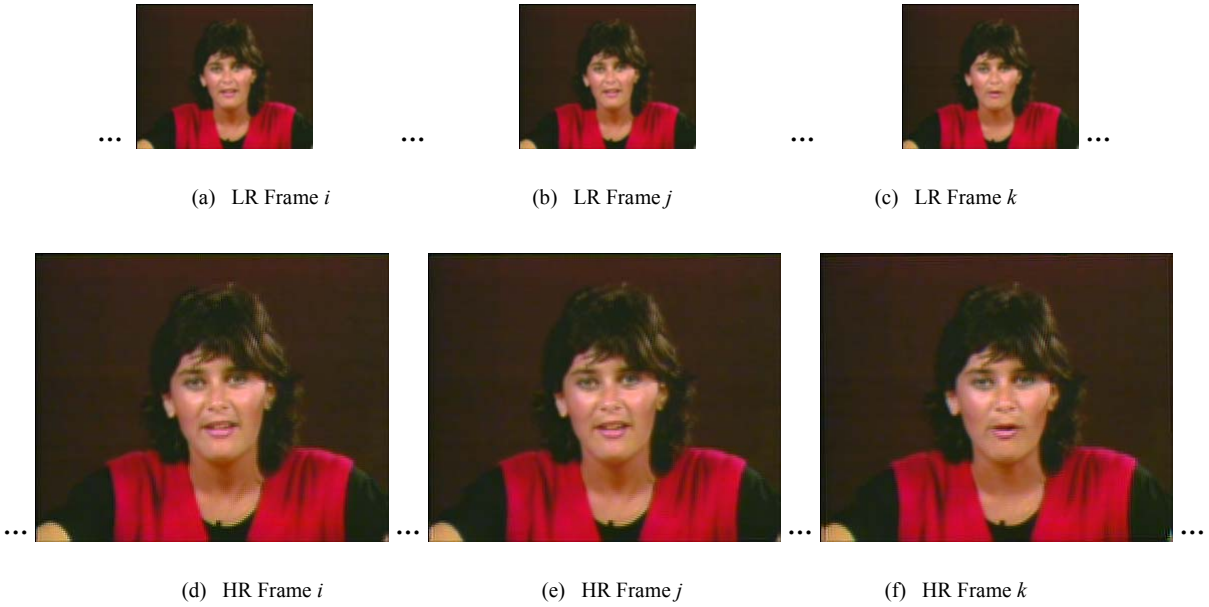

(a) LR Frame *i* (b) LR Frame *j* (c) LR Frame *k*

(d) HR Frame *i* (e) HR Frame *j* (f) HR Frame *k*

Figure 6. Video Ex. 2.

V. Conclusions

In this paper, we give a space-frequency POCS method. The method can be used to super resolution for either images or videos. Comparing with the existing space POCS, our method reduces the edge oscillation artifacts and increases the PSNR of images.

However, to solve the constrained optimization problems, some iteration steps are used. So our method is slow in the implementation. We will consider its acceleration in future work.

Appendix A Matlab Code for affine Parameters

```
% Affine Parameter Calculation  Matlab code
function P = Affine(Image1, Image2, Num);
% Initialization parameter vector
P(1:6) = 0;
for Level = 2:-1:0
    % Get sampling step
    Step = 2.^Level;
    P = [P(1) P(2) P(3) P(4) P(5) P(6)];
    % Compute correlation matrices
    Im1 = Corr(Image1, Step);
    Im2 = Corr(Image2, Step);
    for i=1:3
        % Motion compensate
        Compen = Comp(Im2, P, Num-1);
        % Calculate spatial-temporal gradients
        [Gx Gy Gt] = Grad(Im1, Compen);
        % Calculate increments of parameters
        InP = InParameter(Gx, Gy, Gt, Num);
        % Calculate P
        P = P + InP;
    end
end
```

Acknowledgment

We are very grateful to the referees for their helpful suggestions and comments. This work was partially supported by the TianYuan Special Funds for Mathematics of the National Natural Science Foundation of China (Grant No. 11326243), the National Natural Science Foundation of China (Grant No. 11371174), the Natural Science Foundation of Jiangsu Province of China for Young Scholar (Grant No. BK20130117), the Natural Science Foundation of Zhejiang Province of China (Grant No. LQ13F020003), and the Fundamental Research Funds for the Central Universities of China (Grant No. JUSRP111A18).

References

[1] T. Ahmad and X. Li, "An Integrated Interpolation-based Super Resolution Reconstruction Algorithm for Video Surveillance," *Journal of Communications*, vol. 7, pp. 464-472, June, 2012, doi: 10.4304/jcm.7.6.464-472.

[2] K. Huang, R. Hu, Z. Han, T. Lu, J. Jiang, et al. "Face Image Superresolution via Locality Preserving Projection and Sparse Coding," *Journal of Software*, vol. 8, pp. 2039-2046, August, 2013, doi: 10.4304/jsw.8.8.2039-2046.

[3] X. Li, L. Tian, X. Zhao, and X. Chen, "A Super Resolution Approach for Spectral Unmixing of Remote Sensing Images," *International Journal of Remote Sensing*, vol. 32, pp. 6091-6107, Nov. 2011, doi: 10.1080/01431161.2010.507794.

[4] Z. Yan, Y. Lu, J. Wen and C. Li, "Super Resolution SPECT Reconstruction with Non-uniform Attenuation," *Computer in Biology and Medicine*, vol. 42, pp. 651-656, June, 2012, doi: 10.1016/j.compbiomed.2012.02.005.

[5] C. Chu, "Super-resolution Image Reconstruction for Mobile Devices," Multimedia Systems, vol. 19, pp. 315-337, July, 2013, doi: 10.1007/s00530-012-0276-y.

[6] X. Zhang, M. Tang and R. Tong, "Robust Super Resolution of Compressed Video," *Visual Computer*, vol. 28, pp. 1167-1180, Nov. 2012, doi: 10.1007/s00371-011-0666-8.

[7] W. T. Freeman, T. R. Jones and E. C. Pasztor, "Example-based Super-resolution," *IEEE Computer Graphics and*

© 2014 ACADEMY PUBLISHER

Applications, vol. 22, pp. 56-65, Mar./Apr. 2002, doi: 10.1109/38.988747.
[8] W. Ni, B. Guo and L. Yang, "Example based Super-Resolution Algorithm of Video in Contourlet Domain," *Fourth International Conference on Image and Graphics* (*ICIG 2007*), p.13-19, 2007, doi: 10.1109/ICIG.2007.136.
[9] Z. Xiong, X. Sun and F. Wu, "Robust Web Image/Video Super-resolution," *IEEE Trans. Image Process*, vol. 19, pp. 2017-2028, August, 2010, doi: 10.1109/TIP.2010.2045707.
[10] H. Huang and H. He, "Super-resolution Method for Face Recognition Using Nonbilinear Mappings on Coherent Features," *IEEE Trans. Neural Netw.*, vol. 22, pp. 121-130, Jan., 2011, doi: 10.1109/TNN.2010.2089470.
[11] W. Wu, Z. Liu and X. He, "Learning-based Super Resolution Using Kernel Partial Least Squares," *Image and Vision Computing*, vol. 29, pp. 394-406, May, 2011, doi: 10.1016/j.imavis.2011.02.001.
[12] T. Komatsu, T. Igarashi, K. Aizawa and T. Saito, "Very High Resolution Imaging Scheme with Multiple Different-aperture Cameras," *Signal Processing: Image Communication*, vol. 5, pp. 511-526, Dec., 1993, doi: 10.1016/0923-5965(93)90014-K.
[13] X. Zhang, Y. Liu, "A Computationally Efficient Super-Resolution Reconstruction Algorithm Based On The Hybird Interpolation," *Journal of Computers*, vol. 5, pp. 885-892, June, 2010, doi: 10.4304/jcp.5.6.885-892.
[14] P. Krämer, J. Benois-Pineau and J. P. Domenger, "Local Object-based Super-resolution Mosaicing from Low-resolution Video," *Signal Processing*, vol. 91, pp. 1771-1780, August, 2011, doi: 10.1016/j.sigpro.2011.02.001.
[15] S. Izadpanahi, H. Demirel, "Motion based video super resolution using edge directed interpolation and complex wavelet transform," *Signal Processing*, vol. 93, pp. 2076-2086, July, 2013, doi: 10.1016/j.sigpro.2013.01.006.
[16] H. Stark and P. Oskoui. "High-resolution Image Recovery from Image-plane Arrays, Using Convex Projections," *Journal of the Optical Society of America* (*A*), vol. 6, pp. 1715-1726, Nov., 1989, doi: 10.1364/JOSAA.6.001715.
[17] A. Tekalp, M. Ozkan and M. Sezan, "High-resolution image reconstruction from lower-resolution image sequences and space varying image restoration," 1992 IEEE International Conference on Acoustics, Speech, and Signal Processing, vol. 3, p. 169-172, 1992, doi: 10.1109/ICASSP.1992.226249.
[18] K. Ratakonda and N. Ahuja, "POCS based Adaptive Image Magnification," 1998 International Conference on Image Processing (ICIP 98), vol. 3, p. 203-207, 1998, doi: 10.1109/ICIP.1998.727167.
[19] R. R. Schultz and R. L. Stevenson, "Extraction of High-resolution Frames from Video Sequences," *IEEE Transactions on Image Processing*, vol. 5, pp. 996-1011, June, 1996, doi: 10.1109/83.503915.
[20] G. K. Chantas, N. P. Galatsanos and C. L. Likas, "Bayesian Restoration Using a New Nonstationary Edge-preserving Image Prior," *IEEE Transactions on Image Processing*, vol. 15, pp. 2987-2997, Oct., 2006, doi: 10.1109/TIP.2006.877520.
[21] S. P. Belekos, N. P. Galatsanos and A. K. Katsaggelos, "Maximum a Posteriori Video Super-resolution Using a New Multichannel Image Prior," *IEEE Transactions on Image Processing*, vol. 19, pp. 1451-1464, June, 2010, doi: 10.1109/TIP.2010.2042115.
[22] J. Lu, H. Zhang, Y. Sun, "Video super resolution based on non-local regularization and reliable motion estimation," *Signal Processing: Image Communication*, vol. 29, pp. 514-529, April, 2014, doi: 10.1016/j.image.2014.01.002.
[23] M. Irani and S. Peleg, "Improving Resolution by Image Registration," *CVGIP: Graphical Models and Image Processing*, vol. 53, pp. 231-239, May, 1991, doi: 10.1016/1049-9652(91)90045-L.
[24] B. C. Tom and A. K. Katsaggelos, "Resolution enhancement of monochrome and color video using motion compensation," *IEEE Transactions on Image Processing*, vol. 10, pp. 278-287, Feb., 2001, doi: 10.1109/83.902292.
[25] F. Qin, L. Zhu, L. Cao, W. Yang, "Blind Single-Image Super Resolution Reconstruction with Gaussian Blur and Pepper & Salt Noise," *Journal of Computers*, vol. 9, pp. 896-902, April, 2014, doi: 10.4304/jcp.9.4.896-902.
[26] H. Su, L. Tang, D. Tretter and J. Zhou, "A Practical and Adaptive Framework for Super-resolution," *15th IEEE International Conference on Image Processing*, p. 1236-1239, 2008, doi: 10.1109/ICIP.2008.4711985.
[27] J. Tian and K. Ma, "A Survey on Super-resolution Imaging," Signal, Image and Video Processing, vol. 5, pp. 329-342, Sep. 2011, doi: 10.1007/s11760-010-0204-6.
[28] S. Wang, L. Zhuo, L. Shen, X. Li, "A Least Square Affine-Based Block-Match Image Registration Algorithm for Dynamic Video Super Resolution," *Journal of Electronics & Information Technology*, vol. 31, pp. 542-545, March, 2009, doi: 10.3724/SP.J.1146.2007.01745.

Wanqiang Shen received a Bachelor degree, a Master degree and a PhD degree in Applied Mathematics from Department of Mathematics, Zhejiang University, Hangzhou, China in 2002, 2005 and 2010, respectively.

She has worked as a lecturer in School of Science, Jiangnan University, Wuxi, China since 2011. She was a senior research associate in Department of Manufacturing Engineering and Engineering Management, City University of Hongkong, Hongkong of China, from 2010 to 2011. In 2010, she also joined in Intelligent Video Group of Wuxi Institute of Wireless Sensor Network, Wuxi, China for summer internship. From 2005 to 2007, she worked as a teaching assistant in Department of Information and Computing Science, Changzhou University, Changzhou, China. Her research interests contains digital image processing and geometric modeling.

Lincong Fang received a Bachelor degree and a PhD degree in Applied Mathematics from Institute of Computer Graphic and Image Processing, Department of Mathematics, Zhejiang University, Hangzhou, China in 2004 and 2009, respectively.

He is now a postdoc researcher in LE2I, University of Bourgogne, Dijon, France. He joined School of Information Technology, Zhejiang University of Finance & Economics, Hangzhou, China as an assistant professor in 2012. He worked as a system engineer and project manager in Huawei Technology Co., Ltd., Hangzhou, China during 2010 and 2012. His research interests contains geometric constraints solving, geometric modeling.

© 2014 ACADEMY PUBLISHER

Xiang Chen received a Bachelor degree in Information and Computational Science from School of Science, Jiangnan University, Wuxi, China in 2013.

After graduation, he has worked as a Software Engineer in Department of Research and Development of Shangbo Information Technology Co. Ltd., Wuxi, China. His research interests is digital image processing.

Honglin Xu received a Bachelor degree in Information and Computing Science from School of Science, a PhD degree in Information Technology and Engineering from School of Information Engineering, Jiangnan University, Wuxi, Jiangsu, China in 2003 and 2010 respectively.

She has worked in School of Science, Jiangnan University, Wuxi, Jiangsu, China as a lecture since 2010. Her research interests contains information theory and artificial intelligence.

© 2014 ACADEMY PUBLISHER